Available online at www.sciencedirect.com

ScienceDirect

Signal Processing 88 (2008) 1035–1045

SIGNAL PROCESSING

www.elsevier.com/locate/sigpro

Applications of the SRV constraint in broadband pattern synthesis

Huiping Duan[a,*], Boon Poh Ng[a], Chong Meng Samson See[b], Jun Fang[c]

[a]School of Electrical and Electronic Engineering/NTU-Temasek Laboratories, Nanyang Technological University, Singapore 639798, Singapore

[b]DSO National Laboratories/NTU-Temasek Laboratories, 20 Science Park Drive, Singapore 118230, Singapore

[c]Department of Electrical and Computer Engineering, Stevens Institute of Technology, Hoboken, NJ 07030, USA

Received 20 February 2007; received in revised form 24 October 2007; accepted 7 November 2007
Available online 17 November 2007

Abstract

In this paper, the spatial response variation (SRV) is defined to measure the fluctuation of the array spatial response within the desired frequency band. Applying the SRV constraint in the optimization formulations to produce the frequency invariant beampattern (FIBP) is investigated. An efficient way to formulate the FIBP synthesis problems is proposed. Examples are demonstrated to show the effect of applying the SRV constraint in broadband pattern synthesis.

Keywords: Broadband pattern synthesis; Frequency invariant beampattern (FIBP); Spatial response variation (SRV)

1. Introduction

In applications using sensor arrays to process broadband signals, such as audio teleconferencing using microphone and loudspeaker arrays to process the speech signals, the array beampattern with a constant beamwidth over the frequency band of interest is desired to avoid the effect of lowpass filtering [1,2]. Some applications even require the array spatial response in the whole field of view to remain constant with respect to frequency. A typical example is the multi-beam beamforming network in the beamspace adaptive array [3,4]. As indicated in [3], the frequency invariant property is required in the whole field of view of each beam to prevent distortion of interferences arriving from any direction. The frequency-dependent response will damage the replica of the interference and hence degrade the performance of adaptive beamforming severely. Both the above two types of beampatterns are referred to as the frequency invariant beampattern (FIBP) in literatures.

In order to get a constant beamwidth over the frequency range of interest, the harmonic nesting approach [1,5] uses several subarrays with properly chosen apertures and geometries and combines their outputs in a frequency-dependent way. To further improve the frequency invariance of the beampattern, the filter-and-sum beamformer is used in each subarray in [6]. In [7], the asymptotic theory of unequally spaced arrays is used to derive the

*Corresponding author.
E-mail addresses: duan0002@ntu.edu.sg (H. Duan), ebpng@ntu.edu.sg (B.P. Ng), schongme@dso.org.sg (C.M.S. See), Jun.Fang@stevens.edu (J. Fang).

0165-1684/$ - see front matter
doi:10.1016/j.sigpro.2007.11.001

relationship between the beampattern characteristics and the functional requirements on sensor spacings and weightings. The theory for the far-field frequency invariant beamformer (FIB) presented in [8] offers deep insights into the issue of the FIBP synthesis. Multi-rate and single-rate methods combining the finite impulse response (FIR) or infinite impulse response (IIR) filters are studied in [9,10]. In Refs. [3,4,11], the fan filter is used to produce the FIBP for the uniformly spaced arrays. The design of the FIBP for planar arrays like the concentric ring array and the rectangular array can be found in [12–14]. The superdirective array with the FIBP is studied in [15,16].

Existing designs synthesize the beampattern with the frequency invariant feature in either the whole spatial region [3,8,9] or only the mainlobe directions [1,2,5]. It is desirable to have a method that allows us to specify arbitrary angles at which the spatial response is frequency invariant. Moreover, there is no criterion to measure the extent of the frequency invariance of the synthesized beampattern quantitatively.

In this paper, we propose a spatial response variation (SRV) constrained pattern synthesis method to produce the FIBP. The SRV is defined to measure the fluctuation of the array spatial response over the desired frequency band. By constraining the average SRV in the specified angles to be smaller than a threshold, a desirable tradeoff between the frequency invariance and other characteristics of the beampattern can be obtained. By changing the spatial region specified in the SRV constraint, the frequency invariant feature can be obtained for any direction of interest. Therefore, relative to the existing approaches, the SRV constrained pattern synthesis method shows greater flexibility. Although the SRV is defined in a form which looks like the mean square error, it is completely different from the minimum mean square error method. This will be explained in detail in Section 3 where the definition of the SRV is presented. Besides, an efficient way to formulate the FIBP synthesis problems is investigated. The number of constraints and hence the complexity of the optimization formulations are significantly reduced.

This paper is organized as follows: In Section 2, the mathematical formulations of the array model and the definition of the convex optimization problem are introduced. In Section 3, the definition of the SRV constraint and its applications in broadband pattern synthesis are presented. In Section 4, examples of synthesizing the FIBP are demonstrated. Brief conclusions are drawn in Section 5.

2. Background

For a broadband array with L sensors and J taps connected after each element, the beamforming output is the sum of all the LJ weighted tap signals. The $LJ \times 1$ real-valued weight vector $\boldsymbol{w}$ for the broadband array is defined as follows:

$$\boldsymbol{w} = [w_{1,1} \quad \cdots \quad w_{L,1} \quad \cdots \quad w_{1,J} \quad \cdots \quad w_{L,J}]^{\mathrm{T}}, \tag{1}$$

where the superscript T denotes the transpose. The two-dimensional spatial response is expressed by

$$H(f,\theta) = \boldsymbol{w}^{\mathrm{T}}\boldsymbol{s}(f,\theta). \tag{2}$$

The beampattern is defined as the norm square of the spatial response. $\boldsymbol{s}(f,\theta)$ is the $LJ \times 1$ steering vector which is written as

$$\boldsymbol{s}(f,\theta) = \boldsymbol{s}_T(f) \otimes \boldsymbol{s}_\tau(f,\theta), \tag{3}$$

where $\otimes$ represents the Kronecker product operator, and

$$\boldsymbol{s}_T(f) = [1 \quad \mathrm{e}^{-\mathrm{j}2\pi f T_\mathrm{s}} \quad \cdots \quad \mathrm{e}^{-\mathrm{j}2\pi f (J-1) T_\mathrm{s}}]^{\mathrm{T}}, \tag{4a}$$

$$\boldsymbol{s}_\tau(f,\theta) = [\mathrm{e}^{\mathrm{j}2\pi f \tau_1(\theta)} \quad \mathrm{e}^{\mathrm{j}2\pi f \tau_2(\theta)} \quad \cdots \quad \mathrm{e}^{\mathrm{j}2\pi f \tau_L(\theta)}]^{\mathrm{T}}, \tag{4b}$$

where T_s is the sampling interval of the temporal filter in each channel. $\tau_i(\theta)$ is the propagation delay from the array origin to the ith sensor for the source coming from θ. Arbitrary element responses can be multiplied to the entries of $\boldsymbol{s}_\tau(f,\theta)$ if necessary.

Except some nonconvex synthesis problems, in many scenarios, pattern synthesis can be formulated as convex optimization problems, which in [17] is defined in a standard form as follows:

$$\begin{aligned} \min_{\boldsymbol{x}} \quad & F_0(\boldsymbol{x}) \\ \text{s.t.} \quad & F_i(\boldsymbol{x}) \leqslant 0, \quad i = 1,2,\ldots,m, \\ & \boldsymbol{a}_k^{\mathrm{T}}\boldsymbol{x} = \boldsymbol{b}_k, \quad k = 1,2,\ldots,p, \end{aligned} \tag{5}$$

where $F_0,\ldots,F_m$ are convex functions. $m,p \in \mathbb{Z}^+$. $\boldsymbol{x} \in \mathbb{R}^n$ is the optimization variable. $\boldsymbol{a}_k$ and $\boldsymbol{b}_k$ are vectors with appropriate dimensions defined according to specific problems.

3. Broadband pattern synthesis using the SRV constraint

3.1. Definition of the SRV constraint

The SRV in the direction θ is defined as follows:

$$\mathrm{SRV}(\theta)=\frac{1}{B_\Omega}\int_{f\in\Omega}|\boldsymbol{w}^{\mathrm{T}}\boldsymbol{s}(f,\theta)-\boldsymbol{w}^{\mathrm{T}}\boldsymbol{s}(f_0,\theta)|^2\,\mathrm{d}f. \tag{6}$$

It represents the variation of the spatial response within the frequency range Ω. B_Ω denotes the bandwidth of Ω. f_0 is the reference frequency selected within the frequency range. In definition (6), the template for the desired response is not fixed but a function of the weight vector which is to be optimized. Therefore, the value of the SRV reflects the true fluctuation of the synthesized beampattern at different frequencies. However, in the mean square error method, the fixed template is used as the desired response, which has to be found before formulating the mean square error.

Expression (6) can be re-written as

$$\mathrm{SRV}(\theta)=\boldsymbol{w}^{\mathrm{T}}\boldsymbol{C}(\theta)\boldsymbol{w}, \tag{7}$$

where $\boldsymbol{C}(\theta)$ is an $LJ\times LJ$ matrix:

$$\boldsymbol{C}(\theta)=\frac{1}{B_\Omega}\int_{f\in\Omega}[\boldsymbol{s}(f,\theta)-\boldsymbol{s}(f_0,\theta)]\times[\boldsymbol{s}(f,\theta)-\boldsymbol{s}(f_0,\theta)]^{\mathrm{H}}\,\mathrm{d}f. \tag{8}$$

Because $\boldsymbol{C}(\theta)$ is a Hermitian matrix with nonnegative real eigenvalues and the weight vector $\boldsymbol{w}$ is real-valued, it is easy to prove that

$$\boldsymbol{w}^{\mathrm{T}}\boldsymbol{C}^{\mathrm{H}}(\theta)\boldsymbol{w}=[\boldsymbol{w}^{\mathrm{T}}\boldsymbol{C}^{*}(\theta)\boldsymbol{w}]^{\mathrm{T}}=\boldsymbol{w}^{\mathrm{T}}\boldsymbol{C}^{*}(\theta)\boldsymbol{w}, \tag{9a}$$

$$\boldsymbol{w}^{\mathrm{T}}\boldsymbol{C}(\theta)\boldsymbol{w}=\boldsymbol{w}^{\mathrm{T}}[\boldsymbol{C}(\theta)+\boldsymbol{C}^{\mathrm{H}}(\theta)]\boldsymbol{w}/2=\boldsymbol{w}^{\mathrm{T}}\boldsymbol{C}_{\mathrm{r}}(\theta)\boldsymbol{w}, \tag{9b}$$

where the superscripts H and $*$ represent the conjugate transpose and conjugate, respectively. $\boldsymbol{C}_{\mathrm{r}}(\theta)$ is the real part of $\boldsymbol{C}(\theta)$:

$$\boldsymbol{C}_{\mathrm{r}}(\theta)=\frac{1}{B_\Omega}\int_{f\in\Omega}\mathrm{Re}\{[\boldsymbol{s}(f,\theta)-\boldsymbol{s}(f_0,\theta)][\boldsymbol{s}(f,\theta)-\boldsymbol{s}(f_0,\theta)]^{\mathrm{H}}\}\,\mathrm{d}f, \tag{10}$$

where $\mathrm{Re}\{\cdot\}$ represents the real part of $\{\cdot\}$. If the frequency range Ω is $[f_1,f_{\mathrm{u}}]$, $B_\Omega=f_{\mathrm{u}}-f_1$ and $f_{\mathrm{c}}=(f_{\mathrm{u}}+f_1)/2$, the entries of $\boldsymbol{C}_{\mathrm{r}}(\theta)$ can be derived as the following analytical expression:

$$[\boldsymbol{C}_{\mathrm{r}}(\theta)]_{m,n}=[\boldsymbol{C}_{\mathrm{r}1}]_{m,n}-[\boldsymbol{C}_{\mathrm{r}2}]_{m,n}-[\boldsymbol{C}_{\mathrm{r}3}]_{m,n}+[\boldsymbol{C}_{\mathrm{r}4}]_{m,n}, \tag{11}$$

where

$$[\boldsymbol{C}_{\mathrm{r}1}]_{m,n}=\frac{f_{\mathrm{u}}}{B_\Omega}\,\mathrm{sinc}(2f_{\mathrm{u}}\varsigma_{m,n})-\frac{f_1}{B_\Omega}\,\mathrm{sinc}(2f_1\varsigma_{m,n}), \tag{12a}$$

$$[\boldsymbol{C}_{\mathrm{r}2}]_{m,n}=\left[\frac{f_{\mathrm{u}}}{B_\Omega}\,\mathrm{sinc}(2f_{\mathrm{u}}\varsigma_m)-\frac{f_1}{B_\Omega}\,\mathrm{sinc}(2f_1\varsigma_m)\right]\times\cos(2\pi f_0\varsigma_n)+\mathrm{sinc}(B_\Omega\varsigma_m)\times\sin(2\pi f_{\mathrm{c}}\varsigma_m)\sin(2\pi f_0\varsigma_n), \tag{12b}$$

$$[\boldsymbol{C}_{\mathrm{r}3}]_{m,n}=[\boldsymbol{C}_{\mathrm{r}2}]_{n,m}, \tag{12c}$$

$$[\boldsymbol{C}_{\mathrm{r}4}]_{m,n}=\cos(2\pi f_0\varsigma_{m,n}), \tag{12d}$$

where $\mathrm{sinc}(\alpha)=\sin(\pi\alpha)/\pi\alpha$; $\varsigma_{m,n}=\varsigma_m-\varsigma_n$; $\varsigma_m=\tau_{k_1}(\theta)-i_1T_{\mathrm{s}}, m=i_1L+k_1, k_1=1,2,\ldots,L, i_1=0,1,\ldots,J-1$; $\varsigma_n=\tau_{k_2}(\theta)-i_2T_{\mathrm{s}},\ n=i_2L+k_2, k_2=1,2,\ldots,L, i_2=0,1,\ldots,J-1$.

The SRV averaged over the angles of interest is computed by $\overline{\mathrm{SRV}}=(1/B_{\Theta_{\mathrm{FI}}})\int_{\theta\in\Theta_{\mathrm{FI}}}\mathrm{SRV}(\theta)\,\mathrm{d}\theta$, or in the discrete form $\overline{\mathrm{SRV}}=(1/N)\sum_{i=1}^{N}\mathrm{SRV}(\theta_i)$, where Θ_{FI} denotes the set of directions in which the response variation is considered. $B_{\Theta_{\mathrm{FI}}}$ represents the span of Θ_{FI}. $\theta_i,\ i=1,\ldots,N$ denote the angle grids in Θ_{FI}. According to (7), the average SRV can be re-expressed as $\overline{\mathrm{SRV}}=\boldsymbol{w}^{\mathrm{T}}\overline{\boldsymbol{C}_{\mathrm{r}}}\boldsymbol{w}$, where $\overline{\boldsymbol{C}_{\mathrm{r}}}$ is given by $\overline{\boldsymbol{C}_{\mathrm{r}}}=(1/B_{\Theta_{\mathrm{FI}}})\int_{\theta\in\Theta_{\mathrm{FI}}}\boldsymbol{C}_{\mathrm{r}}(\theta)\,\mathrm{d}\theta$ or $\overline{\boldsymbol{C}_{\mathrm{r}}}=(1/N)\sum_{i=1}^{N}\boldsymbol{C}_{\mathrm{r}}(\theta_i)$. When the average SRV is used as a constraint in the optimization, it is not necessary to use too small grid spacing for the angles due to the correlations between responses in neighbouring directions. If the value of $\overline{\mathrm{SRV}}$ is used as a measure of the quality of the generated beampattern, the grid spacing should be small to get a true evaluation of the performance.

Based on the above definitions, the SRV constraint

$$\boldsymbol{w}^{\mathrm{T}}\overline{\boldsymbol{C}_{\mathrm{r}}}\boldsymbol{w}\leqslant\gamma \tag{13}$$

is designed for the broadband array, where the threshold γ is a small positive constant. This is a quadratic inequality constraint. It can be re-expressed as

$$\|\boldsymbol{L}^{\mathrm{T}}\boldsymbol{w}\|^2\leqslant\gamma, \tag{14}$$

where $\boldsymbol{L}=\boldsymbol{U}\boldsymbol{D}^{1/2}$. $\boldsymbol{D}$ is a diagonal matrix including the nonzero eigenvalues of $\overline{\boldsymbol{C}_{\mathrm{r}}}$. $\boldsymbol{U}$ consists of the corresponding eigenvectors. Therefore, introducing the quadratic inequality constraint (14) will not change the convexity of the problem.

3.2. Applications of the SRV constraint

By constraining the average SRV to be less than a small value, we can restrict the synthesized beampattern at different frequencies to be similar to some extent. On the one hand, this motivates us to constrain the SRV in the optimization to obtain the FIBP. On the other hand, this implies that in optimization formulations for broadband pattern synthesis, the constraints imposed over the whole frequency band of interest have redundancies and can be simplified.

To realize specifications of the beampattern without considering the frequency invariance, a broadband pattern synthesis formulation can be expressed in the form as follows:

$$\begin{aligned} \min_{\boldsymbol{w}} \quad & F_0\langle H(f,\theta)\rangle \\ \text{s.t.} \quad & F_i\langle H(f_m,\theta_n)\rangle \leqslant 0, \quad f_m \in \Omega_{\text{pb}},\ \theta_n \in \Theta_1, \\ & G_k\langle H(f_p,\theta_q)\rangle = 0, \quad f_p \in \Omega_{\text{pb}},\ \theta_q \in \Theta_2, \end{aligned} \tag{15}$$

where $m = 1, \ldots, N(\Omega_{\text{pb}})$, $n = 1, \ldots, N(\Theta_1)$ and $i = 1, \ldots, N(\Omega_{\text{pb}}) \cdot N(\Theta_1)$. $p = 1, \ldots, N(\Omega_{\text{pb}})$, $q = 1, \ldots, N(\Theta_2)$ and $k = 1, \ldots, N(\Omega_{\text{pb}}) \cdot N(\Theta_2)$. Ω_{pb} represents the frequency band of interest. We assume that the bandpass filter is used before array processing to remove the frequency components outside Ω_{pb} [13]. $N(\cdot)$ represents the number of the discrete frequency or angle grids in the numerical treatment. Θ_1 and Θ_2 represent two groups of directional regions. $F_0\langle\cdot\rangle$, $F_i\langle\cdot\rangle$ and $G_k\langle\cdot\rangle$ denote convex functions.

To synthesize the broadband FIBP, the SRV constraint (14) can be supplemented in (15) directly. By choosing the value of γ, the extent of the frequency invariance of the beampattern can be controlled. It should be noted that the high-frequency invariance is obtained at the cost of reduced degrees of freedom for realizing other specifications of the spatial response.

If Θ_{FI} specified in the SRV constraint includes both Θ_1 and Θ_2, the optimization formulation can be expressed in an efficient way:

$$\begin{aligned} \min_{\boldsymbol{w}} \quad & F_0\langle H(f,\theta)\rangle \\ \text{s.t.} \quad & F_i\langle H(f_0,\theta_i)\rangle \leqslant 0, \quad \theta_i \in \Theta_1, \\ & G_k\langle H(f_0,\theta_k)\rangle = 0, \quad \theta_k \in \Theta_2, \\ & \|\boldsymbol{L}^{\mathrm{T}}\boldsymbol{w}\|^2 \leqslant \gamma, \quad \Theta_{\text{FI}} = \Theta_1 \cup \Theta_2, \end{aligned} \tag{16}$$

where $i = 1, \ldots, N(\Theta_1)$ and $k = 1, \ldots, N(\Theta_2)$. The spatial response at frequencies other than f_0 might not exactly satisfy the constraints like (15). However, the deviation is not serious when γ is small enough.

The numbers of constraints in the above formulations are compared as follows. In (15), there are $M_1 = N(\Omega_{\text{pb}}) \cdot [N(\Theta_1) + N(\Theta_2)]$ constraints. If supplementing (14) directly in (15), there are $M_2 = M_1 + 1$ constraints. In (16), there are $M_3 = N(\Theta_1) + N(\Theta_2) + 1$ constraints. We know that $N(\Omega_{\text{pb}}) \gg 1$ in broadband scenarios. $N(\Theta_1) + N(\Theta_2)$ is the number of angle grids where the features of the spatial responses are to be specified. Normally, it is a large value up to tens or hundreds. Therefore, we can draw the conclusion that $M_3 \ll M_1$ and $M_3 \ll M_2$. That is to say, the number of constraints is reduced significantly by the efficient formulation. As most of the involved constraints are quadratic or second-order-cone constraints, the computational complexity of the optimization formulation is reduced significantly with the decreased number of such constraints.

4. Simulation examples

4.1. Example 1: synthesis of the FIBP with the frequency invariance in either the mainlobe region or the whole field of view

This example is designed to show that the proposed method can synthesize the beampattern with the frequency invariant feature in either the mainlobe region or the whole field of view. The influence of various SRV constraints on the characteristics of the synthesized beampattern can be observed.

The simulation on a uniform linear array with 15 sensors and 15 taps per element is performed. The normalized operating frequency band of the array is assumed to be $[0.2, 0.4]$. The sensor spacing is one-half of the wavelength corresponding to the maximum frequency. The look direction is 30° and the sidelobe region is specified to be $[-90^\circ, 15^\circ) \cup (45^\circ, 90^\circ]$.

The MinMax optimization criterion is used to synthesize the beampattern with the uniform sidelobe level. To synthesize the beampattern with the frequency invariant response in the whole field of view, the following formulation is used:

$$\begin{aligned} \min_{\boldsymbol{w}} \quad & \varepsilon \\ \text{s.t.} \quad & \boldsymbol{w}^{\mathrm{T}}\boldsymbol{s}(f_m,\theta_0) = 1, \quad f_m \in \Omega_{\text{pb}}, \\ & |\boldsymbol{w}^{\mathrm{T}}\boldsymbol{s}(f_0,\theta_n)| \leqslant \varepsilon, \quad \theta_n \in \Theta_{\text{sl}}, \end{aligned}$$

$$\|\boldsymbol{w}\| \leqslant \gamma_{\boldsymbol{w}},$$
$$\|\boldsymbol{L}^{\mathrm{T}}\boldsymbol{w}\|^2 \leqslant \gamma, \quad \Theta_{\mathrm{FI}} = [-90^\circ, 90^\circ], \tag{17}$$

where θ_0 is the look direction. Θ_{sl} represents the sidelobe region. The weight-norm constraint $\|\boldsymbol{w}\| \leqslant \gamma_{\boldsymbol{w}}$ is used in order to improve the robustness of the beamformer against the array random error. Θ_{FI} is specified to be the whole field of view with the grid spacing chosen to be 5°. In (17), the look-direction constraints are not implemented in the efficient way in order to achieve the exact unity response.

To achieve the frequency invariant response in the mainlobe region, the optimization formulation (17) is revised in the following way: First, the sidelobe constraint in (17) is replaced by $|\boldsymbol{w}^{\mathrm{T}}\boldsymbol{s}\,(f_m, \theta_n)| \leqslant \varepsilon$, $f_m \in \Omega_{\mathrm{pb}}, \theta_n \in \Theta_{\mathrm{sl}}$; second, Θ_{FI} in the SRV constraint is changed to be $[15^\circ, 45^\circ]$ with the grid spacing chosen to be 5°.

After expressing the above synthesis problems by convex optimization formulations, we use the optimization tool SeDuMi [18] to solve the weight vector $\boldsymbol{w}$. By discretizing the frequency band Ω_{pb} into M grids f_m, $m = 1, 2, \ldots, M$, and the sidelobe region Θ_{sl} into N grids θ_n, $n = 1, 2, \ldots, N$, formulation (17) is expressed in the following dual standard form of the second-order cone programming (SOCP):

$$\max_{\boldsymbol{y}} \quad \boldsymbol{b}^{\mathrm{T}}\boldsymbol{y}$$
$$\text{s.t.} \quad \boldsymbol{c} - \boldsymbol{A}^{\mathrm{T}}\boldsymbol{y} \in \kappa, \tag{18}$$

where κ represents a symmetric cone. $\boldsymbol{b}$ is a constant vector: $\boldsymbol{b} = [-1 \ \ 0 \ \ \cdots \ \ 0]^{\mathrm{T}}$. $\boldsymbol{y}$ includes the optimization variables ε and $\boldsymbol{w}$: $\boldsymbol{y} = [\varepsilon \ \ \boldsymbol{w}^{\mathrm{T}}]^{\mathrm{T}}$. $\boldsymbol{c}$ is defined as

$$\boldsymbol{c} = [c_1 \ \ \cdots \ \ c_M \ \ \boldsymbol{c}_{M+1}^{\mathrm{T}} \ \ \cdots \ \ \boldsymbol{c}_{M+N}^{\mathrm{T}} \ \ \boldsymbol{c}_{M+N+1}^{\mathrm{T}} \ \ \boldsymbol{c}_{M+N+2}^{\mathrm{T}}]^{\mathrm{T}} \tag{19}$$

and $\boldsymbol{A}^{\mathrm{T}}$ is defined as

$$\boldsymbol{A}^{\mathrm{T}} = [\boldsymbol{A}_1 \ \ \cdots \ \ \boldsymbol{A}_M \ \ \boldsymbol{A}_{M+1} \ \ \cdots \ \ \boldsymbol{A}_{M+N} \ \ \boldsymbol{A}_{M+N+1} \ \ \boldsymbol{A}_{M+N+2}]^{\mathrm{T}}. \tag{20}$$

The entries of $\boldsymbol{c}$ and $\boldsymbol{A}^{\mathrm{T}}$ are obtained by re-expressing the constraints in (17) as the zero-cone and quadratic-cone constraints, respectively, as follows:

$$[1] - [0 \ \ \boldsymbol{s}^{\mathrm{H}}(f_m, \theta_0)]\boldsymbol{y} = c_m - \boldsymbol{A}_m^{\mathrm{T}}\boldsymbol{y} \in \{0\}^1, \tag{21a}$$

$$\begin{bmatrix} 0 \\ 0 \end{bmatrix} - \begin{bmatrix} -1 & \boldsymbol{0}^{\mathrm{T}} \\ 0 & -\boldsymbol{s}^{\mathrm{H}}(f_0, \theta_n) \end{bmatrix} \boldsymbol{y} = \boldsymbol{c}_{M+n} - \boldsymbol{A}_{M+n}^{\mathrm{T}}\boldsymbol{y} \in \{Q\}^2, \tag{21b}$$

$$\begin{bmatrix} \gamma_{\boldsymbol{w}} \\ \boldsymbol{0} \end{bmatrix} - \begin{bmatrix} 0 & \boldsymbol{0}^{\mathrm{T}} \\ \boldsymbol{0} & -\boldsymbol{I} \end{bmatrix} \boldsymbol{y} = \boldsymbol{c}_{M+N+1} - \boldsymbol{A}_{M+N+1}^{\mathrm{T}}\boldsymbol{y} \in \{Q\}^{LJ+1}, \tag{21c}$$

$$\begin{bmatrix} \sqrt{\gamma} \\ \boldsymbol{0} \end{bmatrix} - \begin{bmatrix} 0 & \boldsymbol{0}^{\mathrm{T}} \\ \boldsymbol{0} & -\boldsymbol{L}^{\mathrm{T}} \end{bmatrix} \boldsymbol{y} = \boldsymbol{c}_{M+N+2} - \boldsymbol{A}_{M+N+2}^{\mathrm{T}}\boldsymbol{y} \in \{Q\}^{r+1}, \tag{21d}$$

where $\boldsymbol{c}_i$ and $\boldsymbol{A}_i^{\mathrm{T}}$ are equivalent to the constant vectors or matrices on the left side of Eqs. (21a)–(21d). r is the number of columns of $\boldsymbol{L}$. $\{0\}$ and $\{Q\}$ represent the zero cone and quadratic cone, respectively.

By (18)–(21d), the software SeDuMi can be used to solve the convex conic optimization problem (17) easily. The parameter γ should be adjusted if the infeasibility is reported by the optimization tool. Another case for achieving the frequency invariance in the mainlobe region can be written in the dual standard form of the SOCP in the same way.

Figs. 1 and 2 demonstrate the beampatterns for the above two cases, with the reference frequency chosen to be $f_0 = f_1$. In the weight-norm constraint, $\gamma_{\boldsymbol{w}}$ is chosen to be 10. γ in the SRV constraint is chosen to get a desirable tradeoff between the frequency invariance in the specified region and other characteristics of the beampattern such as the sidelobe level. It can be seen that, by using the SRV constraint properly, the beampattern with the frequency invariance in the mainlobe region or the whole field of view can be obtained. When Θ_{FI} in the SRV constraint covers larger directional region, the sidelobe level of the beampattern becomes higher.

4.2. Example 2: construction of the multi-beam beamforming network

In the Griffiths–Jim beamformer proposed in [19], FIR filters with adaptive coefficients are used in each channel of the lower branch to process broadband signals. Large numbers of adaptive weights are required in such a beamformer to get sufficient degrees of freedom. Broadband beam-space adaptive array presented in [3] uses groups of

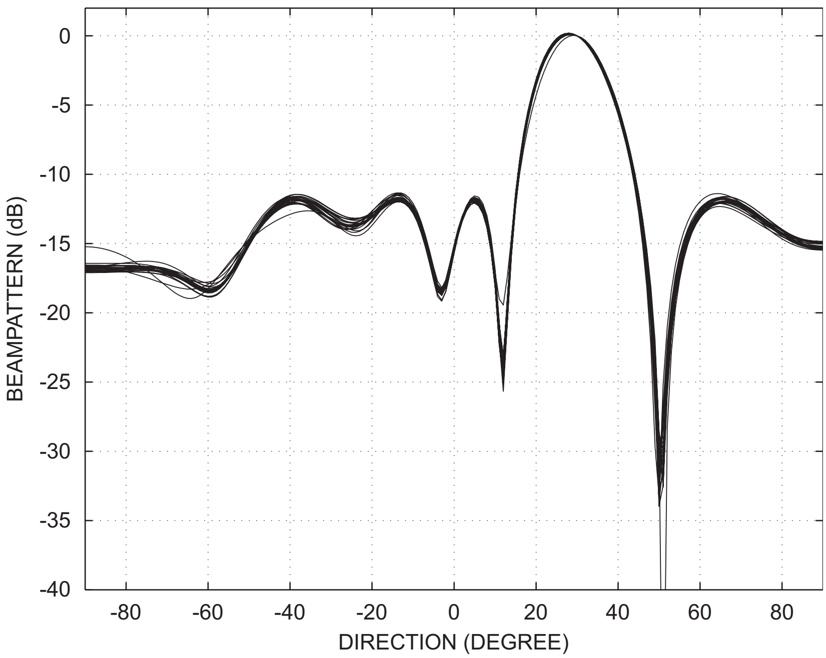

Fig. 1. Beampattern with the frequency invariant response in the whole field of view, at 21 frequencies uniformly distributed within $[0.2, 0.4]$, with $\gamma = 1.0\mathrm{e}-4$.

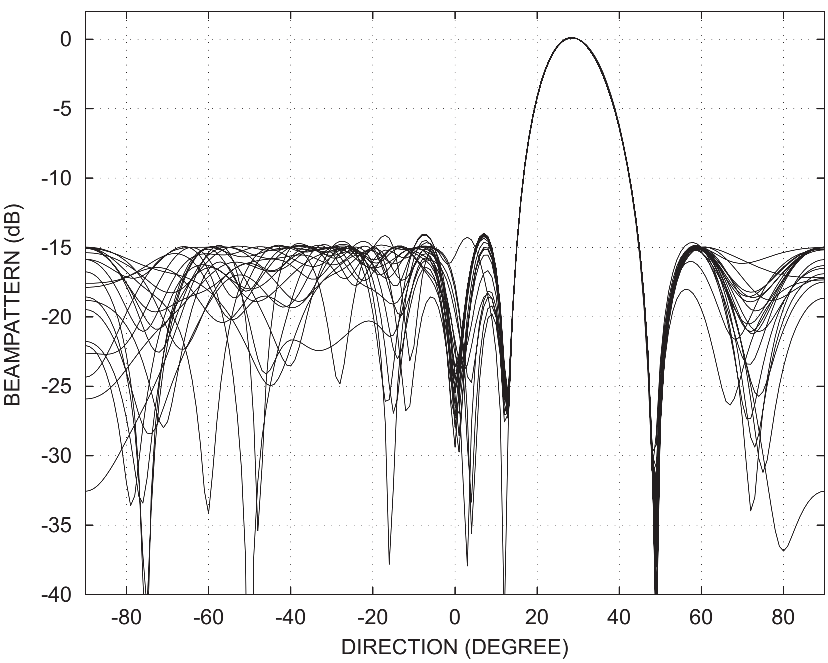

Fig. 2. Beampattern with the frequency invariant response in the mainlobe region, at 21 frequencies uniformly distributed within $[0.2, 0.4]$, with $\gamma = 1.0\mathrm{e}-5$.

fan filters to construct the multi-beam beamforming network. Behind the fixed beamforming network, only a single adaptive weight is required for each beam. Relative to the conventional Griffiths–Jim beamformer, the beamspace adaptive array needs less number of adaptive weights and demonstrates better convergence performance. One thing worth mentioning is that, in broadband beamspace adaptive arrays, frequency invariance in the whole field of view should be guaranteed for the beampattern of each beam. This is to prevent distortion of the broadband interference arriving from any direction, in both the main beam and the auxiliary beams. Since optimization using the SRV constraint can achieve the FIBP in the whole field of view, we utilize the proposed pattern synthesis method to construct the multi-beam beamforming network for the beamspace adaptive array and compare its performance with that of the fan-filter method.

First, based on the idea of the efficient formulation (16), the main beam steered in the look direction θ_0 is designed by the following optimization formulation:

$$\begin{aligned} \min_{\boldsymbol{w}} \quad & \varepsilon \\ \text{s.t.} \quad & \int_{\Omega_{\text{pb}}} |\boldsymbol{w}^{\mathrm{T}}\boldsymbol{s}(f,\theta_0) - 1|^2\,\mathrm{d}f \leqslant 10^{\gamma_m/10}, \\ & |\boldsymbol{w}^{\mathrm{T}}\boldsymbol{s}(f_0,\theta)| \leqslant \varepsilon, \quad \theta \in \Theta_{\text{sl}}, \\ & \|\boldsymbol{w}\| \leqslant \gamma_{\boldsymbol{w}}, \\ & \|\boldsymbol{L}^{\mathrm{T}}\boldsymbol{w}\|^2 \leqslant \gamma, \quad \Theta_{\text{FI}} = [-90^\circ, 90^\circ]. \end{aligned} \tag{22}$$

In (22), the maximum sidelobe level is minimized. The response in θ_0 is constrained to be close to the unity response. γ_m is a small positive constant representing the amplitude of the ripple of the look-direction response. Θ_{FI} for the SRV constraint is specified to be the whole field of view to compute $\boldsymbol{L}$.

Second, the auxiliary beams pointing to θ_i, $i = 1, 2, \ldots, M$, are designed as follows:

$$\begin{aligned} \min_{\boldsymbol{w}} \quad & \varepsilon \\ \text{s.t.} \quad & \int_{\Omega_{\text{pb}}} |\boldsymbol{w}^{\mathrm{T}}\boldsymbol{s}(f,\theta_i) - 1|^2\,\mathrm{d}f \leqslant 10^{\gamma_a/10}, \\ & \int_{\Omega_{\text{pb}}} |\boldsymbol{w}^{\mathrm{T}}\boldsymbol{s}(f,\theta_0) - \delta|^2\,\mathrm{d}f \leqslant 10^{\gamma_m/10}, \\ & |\boldsymbol{w}^{\mathrm{T}}\boldsymbol{s}(f_0,\theta)| \leqslant \varepsilon, \quad \theta \in \Theta_{\text{sl}}, \\ & \|\boldsymbol{w}\| \leqslant \gamma_{\boldsymbol{w}}, \\ & \|\boldsymbol{L}^{\mathrm{T}}\boldsymbol{w}\|^2 \leqslant \gamma, \quad \Theta_{\text{FI}} = [-90^\circ, 90^\circ]. \end{aligned} \tag{23}$$

In this formulation, δ is used to specify a very low gain in the main beam direction to suppress the signal coming from θ_0. γ_a and γ_m are small positive constants representing the amplitudes of the ripples of the response in the directions θ_i and θ_0, respectively. This optimization is carried out once for each auxiliary beam.

Fig. 3 shows the beamspace adaptive array with the structure the same as that presented in [4,6] but

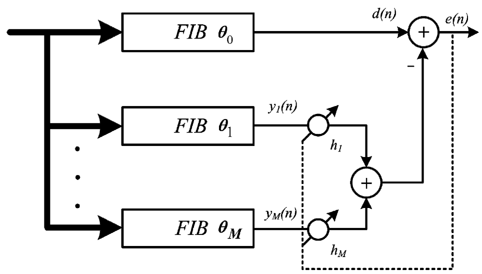

Fig. 3. Broadband beamspace adaptive array using frequency invariant beamformers (FIBs), with the main beam pointing to θ_0 and the auxiliary beams pointing to $\theta_1, \ldots, \theta_M$.

with the multi-beam beamforming network constructed by the weight vectors computed by (22) and (23). The output of the main beam is $d(n)$. A group of adaptive weights h_i are multiplied by the outputs of the auxiliary beams $y_i(n)$. The output of the beamspace adaptive array is $e(n) = d(n) - \boldsymbol{h}^{\mathrm{T}}\boldsymbol{y}(n)$, where $\boldsymbol{h} = [h_1\ h_2\ \cdots\ h_M]^{\mathrm{T}}$ and $\boldsymbol{y}(n) = [y_1(n)\ y_2(n)\ \cdots\ y_M(n)]^{\mathrm{T}}$. The real-valued weight vector $\boldsymbol{h}$ is adjusted by the error signal $e(n)$ with adaptive algorithms.

The simulation scenario is assumed to be as follows: A uniform linear array with 15 isotropic sensors is used. $L = 15$ and $J = 25$ are assumed to generate each beam in the multi-beam beamforming network. The desired signal comes from 0°. Three interferences arrive from −40°, −25° and 30°, respectively. The frequency band for all the directional sources is assumed to be $\Omega_{\text{pb}} = [0.1, 0.3]$. The input signal-to-interference ratio (SIR) for each interference is chosen to be −25 dB. The bandpassed white noise is added to each sensor, with an input signal-to-noise ratio (SNR) of 30 dB.

The fan-filter method proposed in [3] is simulated for the above scenario. According to the studies of [3], first, the values of L and J need to be more than three times the length of the one-dimensional prototype filter to get satisfactory FIBP. Therefore, the length of the lowpass prototype filter is chosen to be equal to 5. Second, with the beams pointing to 0°, ±24° and ±53°, the look direction of each beam nearly coincides with the null directions of the other beams.

In the proposed method, five sets of FIBPs are synthesized, with the main beam pointing to the look direction 0° and four auxiliary beams pointing to ±53° and ±24°, respectively, in order to make it comparable with the fan-filter method. Each auxiliary beam is designed to have a deep null in the look direction of the main beam. The parameters in

(22) and (23) are chosen as follows: $\gamma_m = \gamma_a = -40\,\text{dB}$, $\delta = 0.01$, $\gamma_w = 100$ and $\gamma = 2.0\text{e}-5$. The sidelobe region Θ_{sl} is $[-90^\circ, \theta_0 - 20^\circ] \cup [\theta_0 + 20^\circ, 90^\circ]$ for (22) and $[-90^\circ, \theta_i - 20^\circ] \cup [\theta_i + 20^\circ, 90^\circ]$ for (23). Θ_{FI} is $[-90^\circ, 90^\circ]$. The grid spacings for both Θ_{sl} and Θ_{FI} are chosen to be 5°. Moreover, the normalized least-mean-square (LMS) algorithm [20] is used to compute the adaptive weights. The step size is chosen to be 0.01.

Table 1 lists the values of $\overline{\text{SRV}}$ and the peak sidelobe level (SLL) of the beampatterns averaged over the frequency band for each beam generated by the fan-filter method and the proposed method. We observe that $\overline{\text{SRV}}$ of the beams produced by the proposed method are almost equal to the specified threshold γ. They are always much lower than those achieved by the fan-filter method. This implies much better frequency invariance of the beampatterns. From the values of SLL, we can see that some beams produced by the proposed method have higher SLL than those generated by the fan-filter method, but this does not lead to undesirable interference cancellation performance.

Table 1
Comparison of beams generated by the fan-filter method and the proposed method

Beam	Look direction (deg.)	Fan-filter method		Proposed method	
		$\overline{\text{SRV}}$	SLL (dB)	$\overline{\text{SRV}}$	SLL (dB)
1	0	0.2429	−12.2	2.03e − 5	−20.9
2	−53	0.3787	−10.9	2.01e − 5	−5.5
3	−24	0.2709	−12.0	2.01e − 5	−15.3
4	24	0.2709	−12.0	2.02e − 5	−16.1
5	53	0.3787	−10.9	2.01e − 5	−6.3

Figs. 4 and 5 show the beampatterns of the beamspace adaptive array after 3000 iterations, with the multi-beam beamforming network constructed by the fan-filter method and the proposed method, respectively. The beampatterns averaged over the frequency range [0.1, 0.3] are demonstrated in Fig. 6. Fig. 7 shows the output signal-to-interference-plus-noise ratio (SINR) convergence curves. All the results are obtained by averaging over 200 simulation trials. We observe that the beampattern produced by the proposed method has better frequency invariance and deeper nulls than the fan-filter method. After averaging over Ω_{pb}, the nulling depths in the directions of interferences obtained by the proposed method are −41.4, −41.6

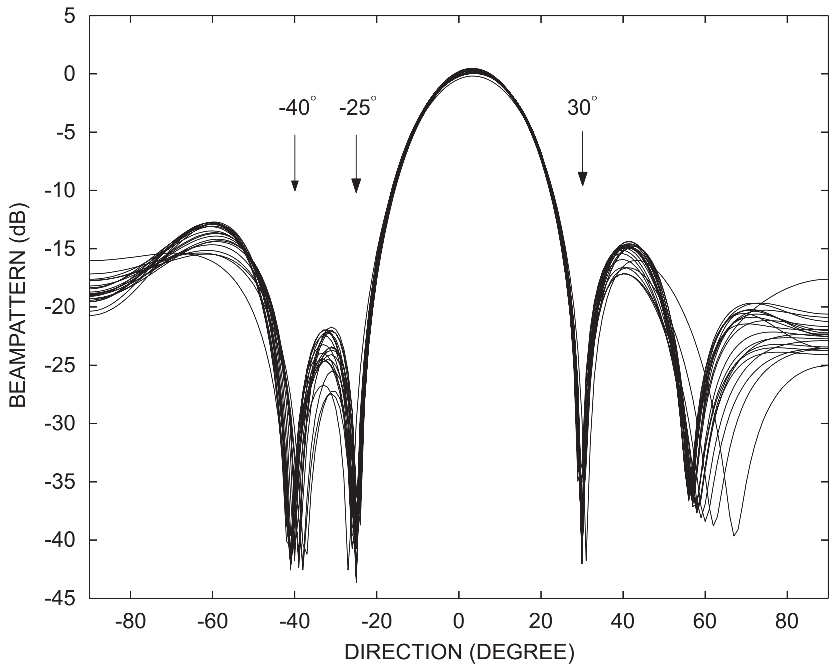

Fig. 4. Beampatterns of the beamspace adaptive array at 21 frequencies uniformly distributed within [0.1, 0.3], with the multi-beam beamforming network constructed by the fan-filter method [3]. The interferences come from -40°, -25° and 30°.

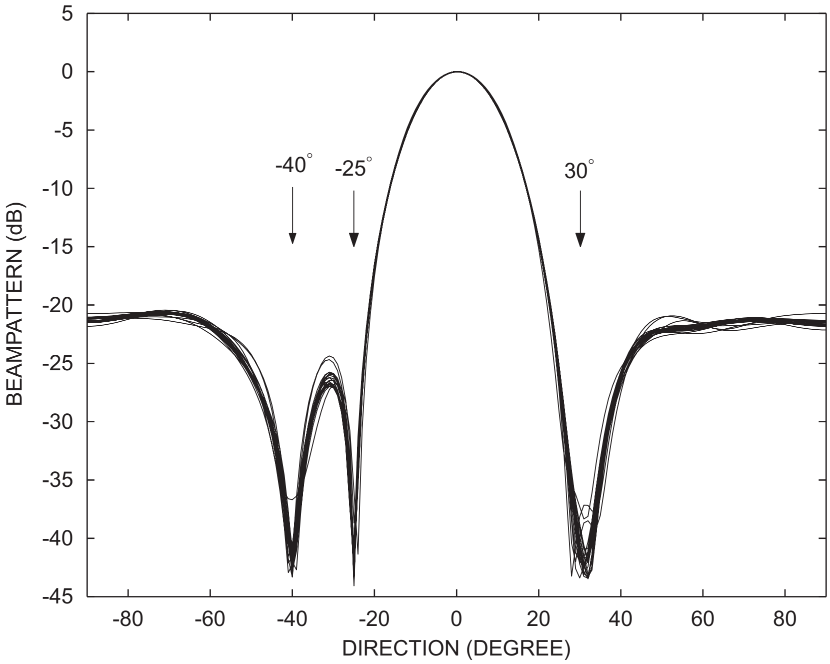

Fig. 5. Beampatterns of the beamspace adaptive array at 21 frequencies uniformly distributed within [0.1, 0.3], with the multi-beam beamforming network constructed by the proposed method. The interferences come from -40°, -25° and 30°.

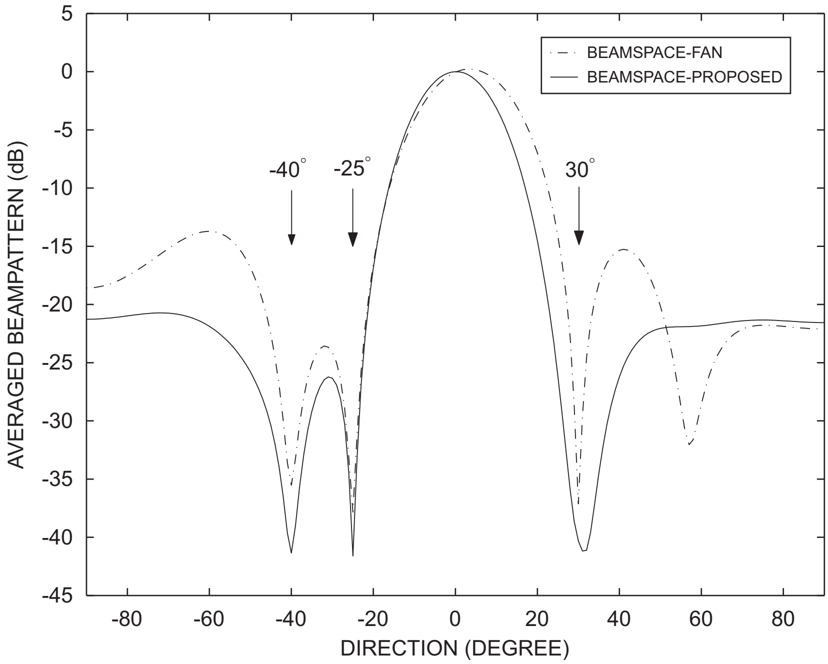

Fig. 6. Beampatterns averaged over [0.1, 0.3] obtained by the fan-filter method and the proposed method.

and $-40.3\,\mathrm{dB}$, while those obtained by the fan-filter method are -35.5, -37.8 and $-37.1\,\mathrm{dB}$, respectively. Moreover, the response in the look direction achieved by the proposed method is closer to the unity response than the fan-filter method. Relative to the fan-filter method, the proposed method

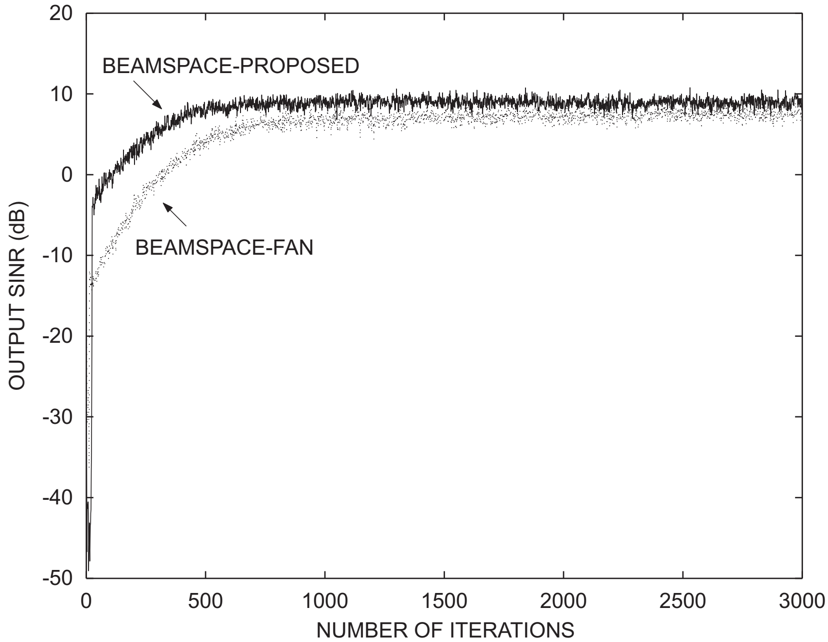

Fig. 7. Output SINR convergence curves of the beamspace adaptive array averaged over 200 trials. The step size is 0.01 in the normalized LMS algorithm.

obtains better output SINR in both the transient state and the steady state.

In the above example, the beams produced by the proposed method show much better frequency invariance. It can be attributed to two reasons: First, the proposed method is able to achieve a desirable tradeoff between the frequency invariance and the sidelobe level of the synthesized beampattern. Second, the assumption of using bandpass filter before array processing reduces the burden of FIBP synthesis. We observe that the good frequency invariance is of great benefit to the improvement of interference cancellation performance in the broadband beamspace adaptive array. It should be noted that, in the proposed method, the values of γ, δ, γ_m and γ_a have a significant influence on the beams. Experiments can be carried out to search good evaluations to produce beampatterns with favourable properties.

Besides the above comparisons, relative to the fan-filter method, the proposed method has some potential superiorities: First, the array geometry is not limited to the uniform spacing. Second, the number of auxiliary beams and the beam directions are not restricted by the prototype filter. With more auxiliary beams, the performance of the beamspace adaptive array can be improved further.

5. Conclusions

In this paper, the SRV constraint is defined to restrict the fluctuation of the spatial response over the desired frequency band for the broadband array. The optimization formulation using the SRV constraint in the efficient way to synthesize the FIBP is studied. Examples are demonstrated to show the effect of applying the SRV constraint in broadband pattern synthesis.

Acknowledgement

The authors would like to acknowledge the anonymous reviewers for their valuable comments and suggestions that helped to improve the quality of this paper.

References

[1] M.M. Goodwin, G.W. Elko, Constant beamwidth beamforming, in: Proceedings of ICASSP-93, vol. 1, April 1993, pp. 27–30.

[2] S. Yan, Optimal design of FIR beamformer with frequency invariant patterns, Appl. Acoust. 67 (6) (June 2006) 511–528.

[3] T. Sekiguchi, Y. Karasawa, Wideband beamspace adaptive array utilizing FIR fan filters for multibeam forming, IEEE Trans. Signal Process. 48 (1) (January 2000) 277–284.

[4] W. Liu, S. Weiss, L. Hanzo, A generalized sidelobe canceller employing two-dimensional frequency invariant filters, IEEE Trans. Antennas Propag. 53 (7) (July 2005) 2339–2343.
[5] E.L. Hixson, K.T. Au, Wide-bandwidth constant beamwidth acoustic array, J. Acoust. Soc. Amer. 48 (1) (1970).
[6] T. Chou, Frequency-independent beamformer with low response error, in: ICASSP, vol. 5, May 1995, pp. 2995–2998.
[7] J.H. Doles III, F.D. Benedict, Broad-band array design using the asymptotic theory of unequally spaced arrays, IEEE Trans. Antennas Propag. vol. 36, no. 1, January 1988, pp. 27–33.
[8] D.B. Ward, R.A. Kennedy, R.C. Williamson, Theory and design of broadband sensor arrays with frequency invariant far-field beam patterns, J. Acoust. Soc. Amer. 97 (February 1995) 1023–1034.
[9] D.B. Ward, R.A. Kennedy, R.C. Williamson, FIR filter design for frequency invariant beamformers, IEEE Signal Process. Lett. 3 (3) (March 1996) 69–71.
[10] S. Forcellini, Frequency invariant beamformer using a single set of IIR filter coefficients, in: IEEE Antennas and Propagation Society International Symposium, vol. 2, June 2002, pp. 563–566.
[11] W. Liu, S. Weiss, J.G. McWhirter, I.K. Proudler, Frequency invariant beamforming for two-dimensional and three-dimensional arrays, Signal Process. 87 (11) (November 2007) 2535–2543.
[12] Y. Li, K.C. Ho, C. Kwan, 3-D array pattern synthesis with frequency invariant property for concentric ring array, IEEE Trans. Signal Process. 54 (2) (February 2006) 780–784.
[13] S.C. Chan, H.H. Chen, Uniform concentric circular arrays with frequency-invariant characteristics-theory, design, adaptive beamforming and DOA estimation, IEEE Trans. Signal Process. 55 (1) (January 2007) 165–177.
[14] M. Ghavami, Wideband smart antenna theory using rectangular array structures, IEEE Trans. Signal Process. 50 (9) (September 2002) 2143–2151.
[15] S. Repetto, A. Trucco, Designing superdirective microphone arrays with a frequency-invariant beam pattern, IEEE Sensors J. 6 (3) (June 2006) 737–747.
[16] A. Trucco, M. Crocco, S. Repetto, A stochastic approach to the synthesis of a robust frequency-invariant filter-and-sum beamformer, IEEE Trans. Instrum. Meas. 55 (4) (August 2006) 1407–1415.
[17] S. Boyd, L. vandenberghe, Convex Optimization, Cambridge University Press, Cambridge, 2004.
[18] J.F. Sturm, Using SeDuMi 1.02, a MATLAB toolbox for optimization over symmetric cones, Optim. Methods Software 11 (1999).
[19] L.J. Griffiths, C.W. Jim, An alternative approach to linearly constrained adaptive beamforming, IEEE Trans. Antennas Propag. 30 (1) (January 1982) 27–34.
[20] S. Haykin, Adaptive Filter Theory, third ed., Prentice-Hall, Englewood Cliffs, NJ, 1996.